Rotary mechanism of V/A-ATPases—how is ATP hydrolysis converted into a mechanical step rotation in rotary ATPases?

Ken Yokoyama*

Department of Molecular Biosciences, Kyoto Sangyo University, Kyoto, Japan

V/A-ATPase is a rotary molecular motor protein that produces ATP through the rotation of its central rotor. The soluble part of this protein, the V_1 domain, rotates upon ATP hydrolysis. However, the mechanism by which ATP hydrolysis in the V_1 domain couples with the mechanical rotation of the rotor is still unclear. Cryo-EM snapshot analysis of V/A-ATPase indicated that three independent and simultaneous catalytic events occurred at the three catalytic dimers (AB_{open}, AB_{semi}, and AB_{closed}), leading to a 120° rotation of the central rotor. Besides the closing motion caused by ATP bound to AB_{open}, the hydrolysis of ATP bound to AB_{semi} drives the 120° step. Our recent time-resolved cryo-EM snapshot analysis provides further evidence for this model. This review aimed to provide a comprehensive overview of the structure and function of V/A-ATPase from a thermophilic bacterium, one of the most well-studied rotary ATPases to date.

KEYWORDS

ATP synthase, V-ATPase, rotary motor protein, molecular motor, FOF1 ATP synthase

Introduction

ATP synthases are enzymes that play crucial roles in energy metabolism (Boyer, 1997; Yoshida et al., 2001; Kuhlbrandt, 2019; Frasch et al., 2022). They convert an electrochemical proton motive force across the membrane generated by respiration into chemical energy that is stored in the form of ATP. In the absence of a proton motive force (*pmf*), ATP synthases can hydrolyze ATP and use the energy released to transport protons across the membrane. Because of this ATP hydrolysis activity, ATP synthases are sometimes referred to as rotary ATPases. ATP synthases are classified into two major categories: F-type ATP synthases (F_oF_1-ATPase) and V-type ATP synthases (V/A-ATPase) (Figures 1A, B) (Yokoyama and Imamura, 2005; Forgac, 2007; Vasanthakumar and Rubinstein, 2020). F_oF_1-ATPases are found in the inner membrane of mitochondria, the thylakoid membrane of chloroplasts, and the plasma membrane of eubacteria (Frasch et al., 2022). V/A-ATPases are present in some eubacteria and archaea and are structurally similar to eukaryotic V-ATPases. The basic structure of both ATPases comprises a rotor complex comprising a hydrophobic c-ring and a stator apparatus surrounding the rotor (Figure 1C). The c-ring in the F_o/V_o domain rotates by the *pmf*, which drives ATP synthesis in the F_1/V_1 domain. Conversely, when ATP is hydrolyzed in the F_1/V_1 domain and the central rotary axis rotates, protons are transported across the membrane in the F_o/V_o domain.
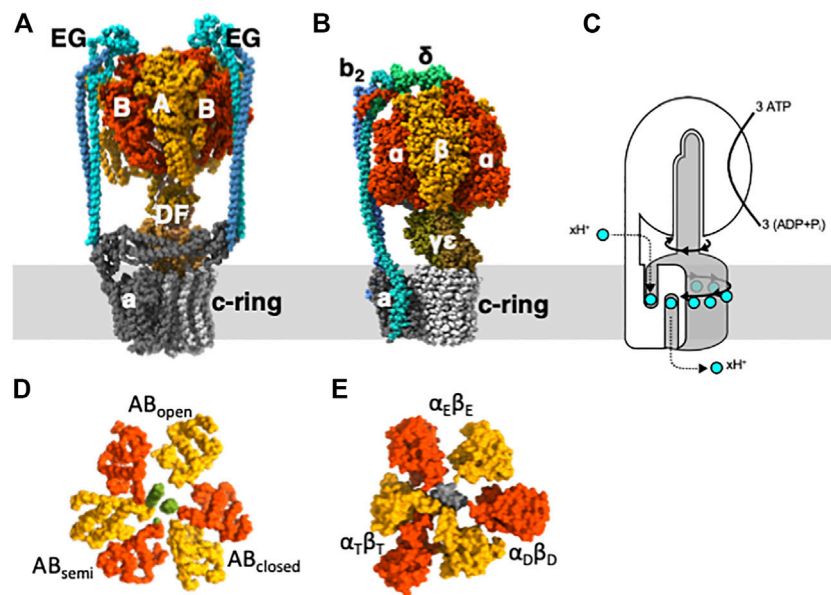
FIGURE 1
Subunit structure and function for V-type and F-type ATPases. **(A)** V/A-ATPase from *Thermus. thermophilus*. **(B)** bacterial F_oF_1 ATPase from *Geobacillus stearothermophilus*. **(C)** The schematic representation illustrates the rotary catalytic mechanism of rotary ATPases, where the rotation of the central rotor complex (grey) driven by ATP in the surrounding stator apparatus (white) rotates the membrane-embedded c-ring, leading to the translocation of protons across the membrane. Slice view of the C-terminal domain of V_1 **(D)** and F_1 **(E)**.
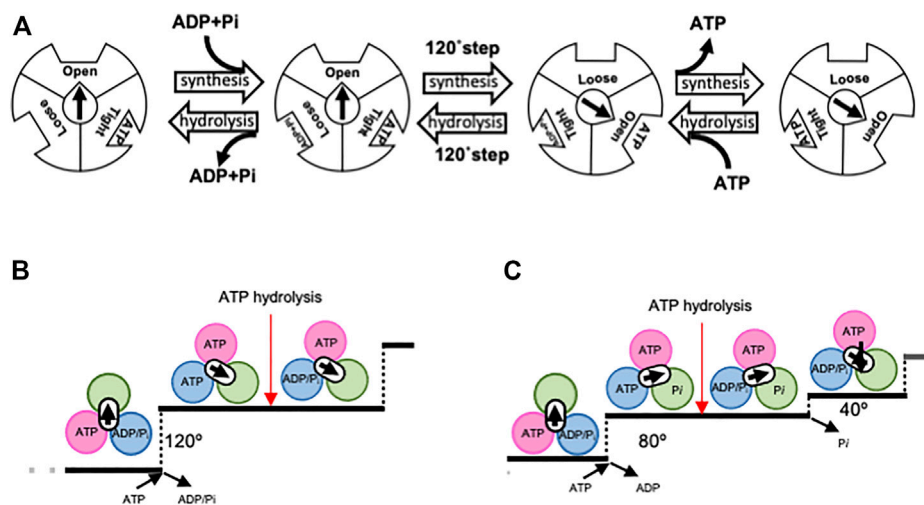

FIGURE 2
Proposed rotary mechanism of rotary ATPases. Boyer first proposed a model for the binding-change mechanism **(A)**. *Open*, *Loose*, and *Tight* bonds correspond to $\alpha_E\beta_E$, $\alpha_D\beta_D$, and $\alpha_T\beta_T$, respectively. The direction of synthesis is characterized by the binding of ADP and Pi to *Loose*, followed by a 120° step that results in *Tight* becoming *Open* and the release of ATP. Through the conversion of *Loose* to *Tight*, ADP is phosphorylated on *Tight* to form ATP. The reverse sequence of events occurred in the direction of ATP hydrolysis. Proposed chemo-mechanical cycles of V_1-ATPase **(B)** and F_1-ATPase **(C)**. Each image was viewed from the V_1/F_1 side. In V_1-ATPase, ATP binding results in a 120° rotation of the DF, followed by ATP hydrolysis. In contrast, F_1-ATPase has been proposed to operate according to a model in which ATP binding initiates an 80° rotation, followed by ATP hydrolysis and Pi release, leading to a further 80° rotation.

The isolated hydrophilic F_1/V_1 domain exhibits ATP hydrolysis activity and is referred to as F_1-ATPase and V_1-ATPase, respectively (Yokoyama et al., 1989; Yokoyama et al., 1990; Weber and Senior, 1997; Suzuki et al., 2016). In the F_1-ATPase, the catalytic site is located at the interface between the α and ß subunits, resulting in three catalytic sites. In V_1-ATPase,

the catalytic site is located at the interface between subunits A and B (Figure 1D) (Maher et al., 2009; Suzuki et al., 2016; Nakanishi et al., 2018). The hydrolysis of a single ATP molecule results in a 120° rotation of the rotor, and the hydrolysis of three ATP molecules results in a full 360° rotation (Imamura et al., 2003).

The theory of the binding change mechanism of F_oF_1-ATPase rotation was proposed by Boyer over 50 years ago (Boyer et al., 1973). This theory postulates that the three catalytic sites within the F_1 domain of F_oF_1-ATPase sequentially adopt *Loose*, *Tight*, and *Open* forms, with differing nucleotide affinities, as the central γ subunit rotates (Figure 2A). Synchronized changes in the properties of these sites lead to ATP release. The asymmetric hexamer structure of the F_1 domain predicted by Boyer was confirmed by the crystal structure of bovine heart mitochondrial F_1-ATPase in 1994 (Abrahams et al., 1994).

The crystal structure of F_1-ATPase revealed that the three catalytic dimers adopted distinct conformations (Figure 1E). One dimer exhibits an open catalytic interface without any nucleotides ($α_Eβ_E$), whereas the other dimer displays a closed structure with ADP bound ($α_Dβ_D$). The third dimer has a partially open structure that accommodates an analog of ATP ($α_Tβ_T$). Since then, numerous crystal structures of F_1-ATPase from different species and under different conditions have been reported, but they are essentially identical to those of asymmetric hexamer (Groth and Pohl, 2001; Menz et al., 2001; Kagawa et al., 2004; Cingolani and Duncan, 2011; Rees et al., 2012; Ferguson et al., 2016).

The rotary catalytic mechanism of F_1-ATPase was directly confirmed by single-molecule observation experiments (Noji et al., 1997). In these experiments, a probe was attached to the rotor γ subunit, whereas the stator $α_3β_3$ was fixed to the glass surface. The rotation of the probe was observed using an optical microscope, and upon ATP addition, the unidirectional rotation of the probe was observed, thereby establishing that F_1-ATPase functions as a rotary molecular motor driven by ATP. Similarly, the rotary mechanism of the V_1-ATPase was demonstrated 5 years later by our group (Imamura et al., 2003).

Since the demonstration of the rotation of F_1-ATPase, numerous single-molecule observation experiments have furthered our understanding of the rotary mechanism of F_1-ATPase (Yasuda et al., 1998; Yasuda et al., 2001; Shimabukuro et al., 2003; Itoh et al., 2004; Adachi et al., 2007; Furuike et al., 2008; Adachi et al., 2012; Saita et al., 2015). For instance, it has been demonstrated that the binding of one ATP molecule results in a 120° step, which comprises an 80° and 40° substep, with ATP hydrolysis occurring at the 80° position (Figures 2B, C) (Yasuda et al., 2001). In addition, high time-resolution analysis has also been performed on F_1-ATPase from *Escherichia coli* using tiny gold rods as probes (Spetzler et al., 2006; Hornung et al., 2011). However, the precise mechanism by which the hydrolysis energy of ATP is converted into rotational force remains unclear.

This review aimed to describe the chemo-mechanical coupling mechanism between ATP hydrolysis and rotor rotation revealed by cryo-snapshot analysis of V/A-ATPase. The similarity between V/A-ATPase and F_oF_1 suggests that the F_1 domain shares this mechanism.

Structure and rotation of V/A-ATPase from *Thermus thermophilus*

The V/A-ATPase from *Thermus thermophilus* is one of the best-studied ATP synthases. It comprises two domains: the V_1 domain and the V_o. The V_1 domain is a rotary motor that rotates its central rotor (DF) within A_3B_3, which contains three catalytic sites comprising AB dimers (Yokoyama and Imamura, 2005; Maher et al., 2009) (Figure 1D).

The V_o domain ($E_2G_2d_1a_1c_{12}$) is composed of stator parts, including *a* subunit and two, EG peripheral stalks, and the d_1c_{12} rotor complex (Kishikawa et al., 2020), which comprises a central rotor complex with the DF subunits of V_1. During the rotation of the central rotor (DF d_1c_{12}), caused by the proton motive force, the DF induces changes in the three AB dimers, leading to the cooperative synthesis of ATP from ADP and Pi at the A_3B hexamer. The reverse rotation of the central rotor caused by ATP hydrolysis by A_3B_3 drives the proton translocation in the V_o domain (Yokoyama et al., 1998; Toei et al., 2007).

A single-molecule rotation experiment showed that the V_1 domain rotates in 120° steps, unlike the 80° steps observed for F_1-ATPases (Figure 2B). This indicates that ATP binding and hydrolysis in the V_1 domain occur at the 120° dwell position (Imamura et al., 2005; Furuike et al., 2011). These results were confirmed by a cryo-EM snapshot analysis.

Structural analysis of V/A- ATPase by cryo-electron microscopy

Although the crystal structures of both F_1-ATPase and V_1-ATPase have been determined, no crystal structures of intact V-ATPase or F_oF_1 have been reported, owing to the structural variability arising from the rotational state of the F_1/V_1 domain.

This situation has changed with the advent of the resolution revolution in cryo-electron microscopy (CryoEM) structural analysis. This has enabled us to obtain the overall structures of F_oF_1 and V-ATPases (Allegretti et al., 2015; Zhao et al., 2015; Zhou et al., 2015; Schep et al., 2016; Nakanishi et al., 2018), and further advances in analytical techniques have made it possible to produce high-resolution maps and build atomic models of rotary ATPases in a relatively short period (Hahn et al., 2018; Roh et al., 2018; Gu et al., 2019; Guo et al., 2019; Murphy et al., 2019; Sobti et al., 2019; Abbas et al., 2020).

The single-particle analysis allowed the separation of different structures present in a V/A-ATPase sample through classification into several classes (Cheng, 2018). In yeast V-ATPase, this technique has led to the isolation of three classes with different orientations of the central rotational axis (Zhou et al., 2015). The same approach was applied to V/A-ATPase, resulting in the isolation of three rotational state structures that showed the significant movement of the peripheral hydrophilic domains (EG and the hydrophilic domain of a subunit) in each state.

To capture the intermediate structure of V/A-ATPase during ATP hydrolysis, we used the TSSA mutant V/A-ATPase, which is less prone to the ADP-inhibited form and has a reduced affinity for ADP at catalytic sites (Nakano et al., 2008). This mutant V/A-ATPase, dialyzed with ethylenediamineetetraacetic acid
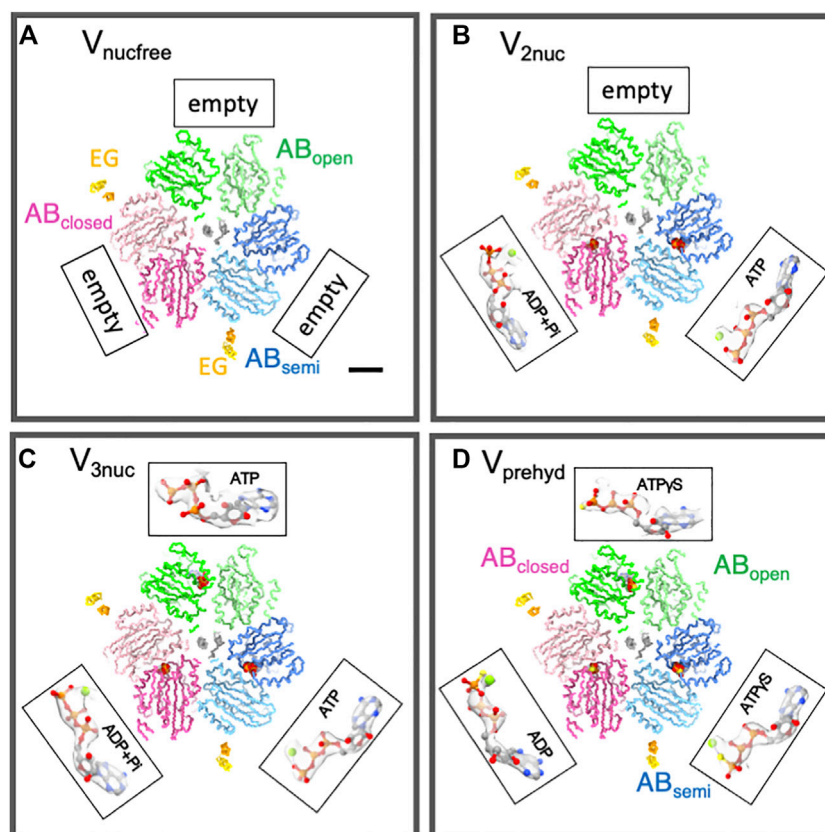
FIGURE 3
Structures of nucleotide binding sites in each condition. The slice of $V_{nucfree}$ **(A)**, V_{prehyd} **(B)**, V_{3nuc} **(C)**, and V_{2nuc} **(D)** viewed from the V_1 (cytosolic) side were shown with bound nucleotides. The scale bar is 20 Å. Three catalytic dimers (AB_{open}, AB_{semi}, and AB_{closed}) in each structure are shown in green, blue, and pink, respectively. Two, EG peripheral stalks were shown in yellow. CryoEM maps were represented as semi-translucent. The magnified view of bound nucleotides and Mg ions was highlighted as a ball-and-stick and sphere representation.

(EDTA)-containing phosphate buffer to remove bound ADP, was reconstituted on nanodiscs and subjected to cryo-grid preparation. We prepared cryogrids under different reaction conditions, such as waiting for ATP binding with a low ATP concentration, waiting for a catalytic reaction with a saturated ATP concentration, and a saturated ATPγS concentration. These samples were then subjected to cryo-electron microscopy using a Titan Krios. The atomic-resolution structures of the V_1 domain without nucleotides at the catalytic sites were obtained through single-particle analysis with focused refinement. The nucleotide-free V_1 structure ($V_{nucfree}$) consisted of an open structure (AB_{open}), a slightly closed structure (AB_{semi}), and a closed structure (AB_{closed}) (Figure 3A). The $V_{nucfree}$ structures were largely similar to the V_1 structures occupied by nucleotides at three catalytic sites (V_{3nuc}), implying that the asymmetry of the V_1 domain arises from its intrinsic structure rather than conformational changes induced by nucleotide binding. This asymmetric structure of the V_1 domain has been reported for other V-ATPases (Oot et al., 2016; Suzuki et al., 2016; Abbas et al., 2020; Tan et al., 2022), highlighting the robustness of the V_1 domain structure.

Subsequently, we performed a single-particle analysis of V/A-ATPase in a reaction solution containing 50 μM or 6 mM ATP, and an ATP regeneration system. Given that ATP binding

is the rate-limiting step in the ATP hydrolysis reaction containing 50 μM ATP (which is lower than its K_m of 500 μM), most of the V/A-ATPase molecules in the reaction solution are in a waiting state for ATP binding. The V_1 domain structure under these conditions was largely indistinguishable from that of $V_{nucfree}$, comprising AB_{open}, AB_{semi}, and AB_{closed} structures. Among the catalytic sites, ADP was bound to AB_{closed} and ATP to AB_{semi}, whereas AB_{open} had no bound nucleotide (Figure 3B), suggesting that the next ATP molecule should bind to AB_{open}. This structure was referred to as V_{2nuc} as it contained two bound nucleotides.

In the presence of 6 mM ATP ($>> K_m$), the dwell time for ATP binding to the enzyme was negligible, and most of the V/A-ATPase molecules in the reaction solution were in a waiting state for the catalytic reaction after ATP binding. The V_1 domain under these conditions consisted of AB_{open}, AB_{semi}, and AB_{closed}, all of which were bound to nucleotides (V_{3nuc}) (Figure 3C). AB_{closed} was bound to ATP or (ADP + Pi), while ATP binding was also confirmed at both AB_{open} and AB_{semi}. Therefore, it is clear that ATP will bind to the AB_{open} in the V_{2nuc}, resulting in V_{3nuc} formation. This indicates that the V_{3nuc} represents the state just before the 120° rotation of the rotor takes place. In summary, the 120° rotation does not occur immediately after ATP binds to the V_{2nuc}.
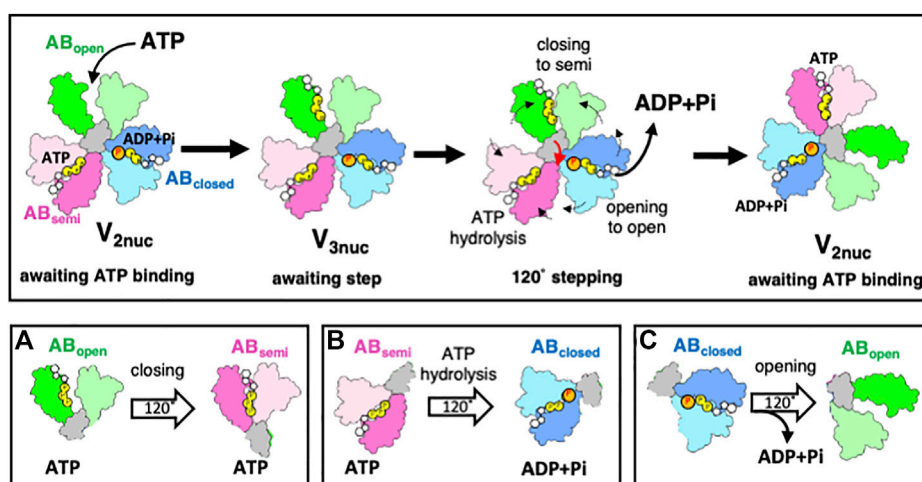
FIGURE 4
The rotary mechanism of the V_1 domain powered by ATP hydrolysis. The figure shows schematic models of AB_{open}, AB_{semi}, and AB_{closed} in green, pink, and blue respectively. The grey region shows the coiled region of the D subunit in contact with A_3B_3. In the V_{2nuc} state, waiting for ATP binding, binding of ATP onto AB_{open} does not result in a 120° step. In the V_{3nuc} state, both the closing of AB_{open} and ATP hydrolysis in AB_{semi} result in the opening of AB_{closed}, accompanied by ADP and Pi release. The catalytic events in three AB dimers occur simultaneously with a 120° step of DF, leading to a structural transition from V_{3nuc} to V_{2nuc}. The lower part of the figure illustrates the simultaneous occurrence of catalytic events at the three catalytic dimers (AB_{open}, AB_{semi}, AB_{closed}) with a 120° step. The events involve changing AB_{open} to AB_{semi} by binding ATP **(A)**. The AB_{semi} also changes AB_{closed} through the hydrolysis of bound ATP **(B)**. AB_{closed} changes AB_{open} through a 120° step of DF, releasing bound ADP and Pi **(C)**.

Finally, a single-particle analysis of V/A-ATPase was performed in a reaction solution containing 4 mM ATPγS, a slow-hydrolyzing ATP analog. Under these conditions, the reaction solution was substrate-saturated; therefore, most of the resulting structures were those waiting for ATP hydrolysis (V_{prehyd}). In V_{prehyd}, ATPγS and ADP were observed at all catalytic sites in the V_1 domain of V/A-ATPase (Figure 3D). Notably, ADP was found at AB_{closed}, indicating that ATPγS-bound AB_{closed} had already been hydrolyzed. This also indicated that ATPγS bound to AB_{semi} was waiting for hydrolysis. In the catalytic site of AB_{semi}, the amino acid residues responsible for ATP hydrolysis were located further away from the ATP molecule (in this case, ATPγS), resulting in a slower ATPγS-bound AB_{semi} hydrolysis. The hydrolysis of ATPγS bound to AB_{semi} requires a conformational change from AB_{semi} to AB_{closed}, which involves 120° rotation in the DF rotor. Thus, V_{prehyd} represents a waiting state for the hydrolysis of ATPγS on AB_{semi} with 120° rotation.

The rotary mechanism of V/A-ATPase fueled by ATP

The structures of the $V_{nucfree}$ and the nucleotide-containing forms (V_{2nuc} and V_{3nuc}) were nearly identical (Figure 3). The asymmetric structure of the V_1 domain, composed of AB_{open}, AB_{semi}, and AB_{closed}, was maintained regardless of the nucleotide-binding state, suggesting that nucleotide binding to the V_1 domain does not cause an asymmetric change in its structure. The conformational changes in the V_1 domain coupled with ATP hydrolysis appear to be discrete, indicating that the power-stroke model, in which the axis rotation is driven by

conformational changes in the catalytic subunit, may not be appropriate.

Previous single-molecule rotation experiments on both F_1-ATPase and V_1-ATPase indicated that the 120° step (80° step in F_1) was concurrent with ATP binding, as the histogram analysis of the initiation dwell time indicated a first-order exponential relationship with ATP concentration (Yasuda et al., 2001; Furuike et al., 2011). The presence of the V_{3nuc} structure, in which ATP is bound but the 120° step has not yet occurred, challenges the assumption that ATP binding to the V_1 domain and the 120° step occur simultaneously.

Structural analysis of V/A-ATPase during rotation provides key insights into the coupling of ATP hydrolysis with the mechanical movement of the rotor. During the transition from V_{3nuc} to V_{2nuc}, the three AB dimers undergo the following conformational changes, as depicted in Figure 4: (a) from AB_{open} to AB_{semi}, (b) from AB_{semi} to AB_{closed}, and (c) from AB_{closed} to AB_{open}, which are accompanied by a 120° step in the DF rotor. (a) Is the process by which the AB dimer becomes more closed upon ATP binding. This has been confirmed experimentally, with the ß-subunit of F_1 showing a closed conformation upon ATP binding (Akutsu, 2017). The difference in the nucleotide states bound to AB_{semi} (ATP) and AB_{closed} (ADP and Pi) generates a downhill chemical potential, which drives the 120° step in the process (b) as the AB dimer changes from AB_{semi} to AB_{closed}. The release of bound ADP and Pi from AB_{closed} and its conversion to AB_{open} during the process (c) is a result of the interaction between ADP or Pi and the amino acid residues at the catalytic site being cleaved, causing AB_{closed} to open (Kishikawa et al., 2022). This process is non-spontaneous and requires external work. If ADP is bound to AB_{closed}, it results in an ADP-inhibited state of the V_1 domain (Yokoyama et al., 1998; Nakanishi et al.,
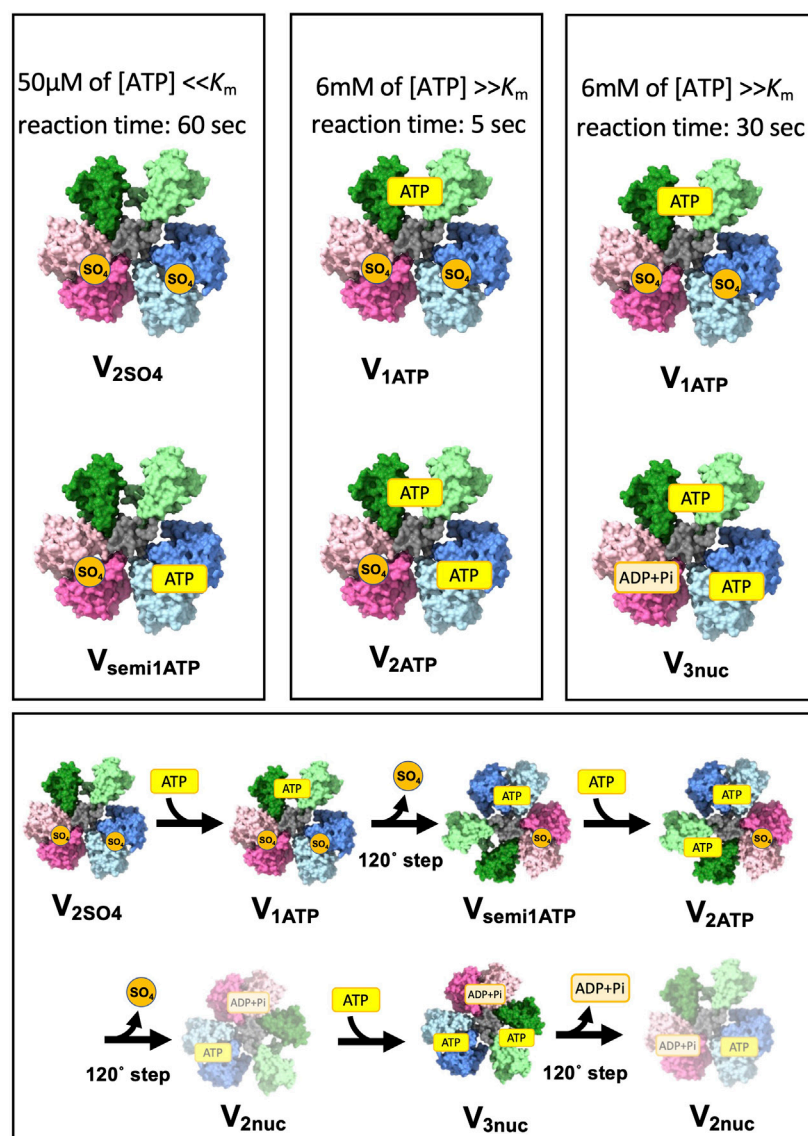
FIGURE 5
Short-lived initial intermediate V_1 structure captured by a time-resolved cryo snapshot analysis. This figure shows the results of cryo-electron microscopy (CryoEM) analysis of the structural changes in a nucleotide-depleted V/A-ATPase enzyme upon reaction with different ATP concentrations. The upper columns represent the initial intermediate structures captured at different time points after the reaction with either 50 μM or 6 mM ATP. The lower column shows the structural transition from the initial intermediate structures to the final, steady-state structures (V_{2nuc} and V_{3nuc}).

2018), and the 120° step does not occur even if ATP is bound to AB_{open}.

Our model represents an improvement over Boyer's original model. Unlike Boyer's bi-site model, which alternates between a state of one and two bound nucleotides and is characterized by a 120° step caused by bound ATP (Figure 2A), the model proposed here is a tri-site model that involves the cooperative interaction of chemical reactions occurring at three distinct sites. This study also sheds light on the role of ATP binding and hydrolysis in the different conformational states of the AB dimer that drives the 120°step of the DF rotor in V/A-ATPase. Both the closure of AB_{open} to AB_{semi} by binding ATP and the hydrolysis of ATP in AB_{semi} trigger the opening of AB_{closed}, leading to ADP and Pi

release from the catalytic site. This process was synchronized with 120°rotation of the DF rotor. This model highlights the coupling between the downhill chemical potential generated by ATP hydrolysis and the mechanical 120° step of the rotor, as confirmed by the time-resolved structural analysis in the following chapter.

Time-resolved snapshot structural analysis of V/A-ATPase

The change in V/A-ATPase from a nucleotide-depleted state to a steady state with nucleotides was studied using the single-

particle cryo-EM method. The experiments were performed as shown in Figure 5. V/A-ATPase reacted with a low concentration of ATP and 20 mM sulfate ions for 60 s (Figure 5A), followed by cryo-grid preparation. The resulting structure ($V_{semi1ATP}$) showed ATP binding to AB_{semi} and a 120° rotation, as indicated by the absence of ATP binding to AB_{open}. The reaction solution containing V/A-ATPase was then reacted with high ATP concentrations for 5 and 30 s. The 5-s reaction solution yielded two structures, V_{1ATP} and V_{2ATP}, with ATP/ ADP and sulfate bound to different sites (Figure 5B). V_{1ATP} showed ATP binding to the catalytic site on AB_{open} and sulfate binding to both AB_{closed} and AB_{semi}. V_{2ATP} contains two ATP molecules in the catalytic sites on AB_{open} and AB_{semi} and sulfate in the catalytic site on AB_{closed}. The 30-s reaction solution yielded two structures, V_{1ATP} and V_{3ATP}, with ATP/ADP bound to all three sites, which is similar to the V_{3nuc} obtained under high ATP conditions in a previous study (Figure 5C).

The transition process from the initial state of V_1 to the V_{3nuc} is shown in Figure 5D. When ATP binds to V_{2SO4}, it changes to V_{1ATP}. Upon ATP binding to AB_{open}, resulting in a 120° step, one molecule of SO_4 is released, resulting in the transition to $V_{semi1ATP}$. ATP binds to $V_{semi1ATP}$ to produce V_{2ATP}. This undergoes a 120° step and releases ADP and Pi, yielding V_{2nuc}. ATP binding to the V_{2nuc} produces V_{3nuc}. The initially bound SO_4 is released, and V_1 eventually reaches a steady state in which V_{2nuc} and V_{3nuc} alternately appear as a result of ATP hydrolysis.

The presence of V_{1ATP} in the 30-s dataset and the absence of V_{2ATP} suggest that an immediate transition from V_{2ATP} to V_{3ATP} occurred. These results suggest that 120° rotation of the rotor does not occur immediately upon the closure of AB_{open} with ATP in the absence of ATP binding on AB_{semi}. This is consistent with our model, in which both the closure of AB_{open} with ATP and the hydrolysis of ATP in AB_{semi} drive the open motion of AB_{closed}, releasing ADP and Pi coupled with the simultaneous 120° rotation of the rotor.

Conclusion

The thermophilic F_1-ATPase has been studied using single-molecule rotation observations, which have shown the presence of at least one intermediate state during the 120° step, in addition to the three rotational states. A recent cryo-electron microscopy (EM) structural study of F_1-ATPase revealed six structures corresponding to these intermediate states (Sobti et al., 2021). The V_1 domain comprises only the basic structures of AB_{open}, AB_{semi}, and AB_{closed}, while the βα dimer, the catalytic unit of F_1-ATPase, adopts intermediate structures beyond these basic structures. This makes the rotational mechanism of the F_1-ATPase more complex than that of the V/A-ATPase, but the

underlying principle remains the same. Our recent structural snapshot analysis of F_oF_1 supports this, suggesting that F_oF_1 converts the downhill chemical potential generated by ATP hydrolysis into a mechanical step through a similar mechanism (Nakano et al., 2022). This highlights the importance of both ATP binding and hydrolysis in the generation of rotational forces by rotary ATPases.

Conflict of interest

The author declares that the research was conducted in the absence of any commercial or financial relationships that could be construed as a potential conflict of interest.

Publisher's note

References

Abbas, Y. M., Wu, D., Bueler, S. A., Robinson, C. V., and Rubinstein, J. L. (2020). Structure of V-ATPase from the mammalian brain. *Science* 367, 1240–1246. doi:10.1126/science.aaz2924

Abrahams, J. P., Leslie, A. G., Lutter, R., and Walker, J. E. (1994). Structure at 2.8 A resolution of F1-ATPase from bovine heart mitochondria. *Nature* 370, 621–628. doi:10.1038/370621a0

Adachi, K., Oiwa, K., Nishizaka, T., Furuike, S., Noji, H., Itoh, H., et al. (2007). Coupling of rotation and catalysis in F(1)-ATPase revealed by single-molecule imaging and manipulation. *Cell* 130, 309–321. doi:10.1016/j.cell.2007.05.020

Adachi, K., Oiwa, K., Yoshida, M., Nishizaka, T., and Kinosita, K., Jr. (2012). Controlled rotation of the F₁-ATPase reveals differential and continuous binding changes for ATP synthesis. *Nat. Commun.* 3, 1022. doi:10.1038/ncomms2026

Akutsu, H. (2017). Dynamic mechanisms driving conformational conversions of the beta and epsilon subunits involved in rotational catalysis of F1-ATPase. *Proc. Jpn. Acad. Ser. B Phys. Biol. Sci.* 93, 630–647. doi:10.2183/pjab.93.040

Allegretti, M., Klusch, N., Mills, D. J., Vonck, J., Kühlbrandt, W., and Davies, K. M. (2015). Horizontal membrane-intrinsic α-helices in the stator a-subunit of an F-type ATP synthase. *Nature* 521, 237–240. doi:10.1038/nature14185

Boyer, P. D., Cross, R. L., and Momsen, W. (1973). A new concept for energy coupling in oxidative phosphorylation based on a molecular explanation of the oxygen exchange reactions. *Proc. Natl. Acad. Sci. U. S. A.* 70, 2837–2839. doi:10.1073/pnas.70.10.2837

Boyer, P. D. (1997). The ATP synthase-a splendid molecular machine. *Annu. Rev. Biochem.* 66, 717–749. doi:10.1146/annurev.biochem.66.1.717

Cheng, Y. (2018). Single-particle cryo-EM-How did it get here and where will it go. *Science* 361, 876–880. doi:10.1126/science.aat4346

Cingolani, G., and Duncan, T. M. (2011). Structure of the ATP synthase catalytic complex (F(1)) from *Escherichia coli* in an autoinhibited conformation. *Nat. Struct. Mol. Biol.* 18, 701–707. doi:10.1038/nsmb.2058

Ferguson, S. A., Cook, G. M., Montgomery, M. G., Leslie, A. G., and Walker, J. E. (2016). Regulation of the thermoalkaliphilic F1-ATPase from Caldalkalibacillus thermarum. *Proc. Natl. Acad. Sci. U. S. A.* 113, 10860–10865. doi:10.1073/pnas.1612035113

Forgac, M. (2007). Vacuolar ATPases: Rotary proton pumps in physiology and pathophysiology. *Nat. Rev. Mol. Cell Biol.* 8, 917–929. doi:10.1038/nrm2272

Frasch, W. D., Bukhari, Z. A., and Yanagisawa, S. (2022). F_1F_O ATP synthase molecular motor mechanisms. *Front. Microbiol.* 13, 965620. doi:10.3389/fmicb.2022.965620

Furuike, S., Hossain, M. D., Maki, Y., Adachi, K., Suzuki, T., Kohori, A., et al. (2008). Axle-less F1-ATPase rotates in the correct direction. *Science* 319, 955–958. doi:10.1126/science.1151343

Furuike, S., Nakano, M., Adachi, K., Noji, H., Kinosita, K., and Yokoyama, K. (2011). Resolving stepping rotation in Thermus thermophilus H(+)-ATPase/synthase with an essentially drag-free probe. *Nat. Commun.* 2, 233. doi:10.1038/ncomms1215

Groth, G., and Pohl, E. (2001). The structure of the chloroplast F1-ATPase at 3.2 A resolution. *J. Biol. Chem.* 276, 1345–1352. doi:10.1074/jbc.M008015200

Gu, J., Zhang, L., Zong, S., Guo, R., Liu, T., Yi, J., et al. (2019). Cryo-EM structure of the mammalian ATP synthase tetramer bound with inhibitory protein IF1. *Science* 364, 1068–1075. doi:10.1126/science.aaw4852

Guo, H., Suzuki, T., and Rubinstein, J. L. (2019). Structure of a bacterial ATP synthase. *Elife* 8, e43128. doi:10.7554/eLife.43128

Hahn, A., Vonck, J., Mills, D. J., Meier, T., and Kuhlbrandt, W. (2018). Structure, mechanism, and regulation of the chloroplast ATP synthase. *Science* 360, eaat4318. doi:10.1126/science.aat4318

Hornung, T., Martin, J., Spetzler, D., Ishmukhametov, R., and Frasch, W. D. (2011). Microsecond resolution of single-molecule rotation catalyzed by molecular motors. *Methods Mol. Biol.* 778, 273–289. doi:10.1007/978-1-61779-261-8_18

Imamura, H., Nakano, M., Noji, H., Muneyuki, E., Ohkuma, S., Yoshida, M., et al. (2003). Evidence for rotation of V1-ATPase. *Proc. Natl. Acad. Sci. U. S. A.* 100, 2312–2315. doi:10.1073/pnas.0436796100

Imamura, H., Takeda, M., Funamoto, S., Shimabukuro, K., Yoshida, M., and Yokoyama, K. (2005). Rotation scheme of V1-motor is different from that of F1-motor. *Proc. Natl. Acad. Sci. U. S. A.* 102, 17929–17933. doi:10.1073/pnas.0507764102

Itoh, H., Takahashi, A., Adachi, K., Noji, H., Yasuda, R., Yoshida, M., et al. (2004). Mechanically driven ATP synthesis by F1-ATPase. *Nature* 427, 465–468. doi:10.1038/nature02212

Kagawa, R., Montgomery, M. G., Braig, K., Leslie, A. G., and Walker, J. E. (2004). The structure of bovine F1-ATPase inhibited by ADP and beryllium fluoride. *Embo J.* 23, 2734–2744. doi:10.1038/sj.emboj.7600293

Kishikawa, J. I., Nakanishi, A., Furuta, A., Kato, T., Namba, K., Tamakoshi, M., et al. (2020). Mechanical inhibition of isolated V(o) from V/A-ATPase for proton conductance. *Elife* 9, e56862. doi:10.7554/eLife.56862

Kishikawa, J., Nakanishi, A., Nakano, A., Saeki, S., Furuta, A., Kato, T., et al. (2022). Structural snapshots of V/A-ATPase reveal the rotary catalytic mechanism of rotary ATPases. *Nat. Commun.* 13, 1213. doi:10.1038/s41467-022-28832-5

Kuhlbrandt, W. (2019). Structure and mechanisms of F-type ATP synthases. *Annu. Rev. Biochem.* 88, 515–549. doi:10.1146/annurev-biochem-013118-110903

Maher, M. J., Akimoto, S., Iwata, M., Nagata, K., Hori, Y., Yoshida, M., et al. (2009). Crystal structure of A3B3 complex of V-ATPase from Thermus thermophilus. *EMBO J.* 28, 3771–3779. doi:10.1038/emboj.2009.310

Menz, R. I., Walker, J. E., and Leslie, A. G. (2001). Structure of bovine mitochondrial F(1)-ATPase with nucleotide bound to all three catalytic sites: Implications for the mechanism of rotary catalysis. *Cell* 106, 331–341. doi:10.1016/s0092-8674(01)00452-4

Murphy, B. J., Klusch, N., Langer, J., Mills, D. J., Yildiz, Ö., and Kühlbrandt, W. (2019). Rotary substates of mitochondrial ATP synthase reveal the basis of flexible F1-Fo coupling. *Science* 364, eaaw9128. doi:10.1126/science.aaw9128

Nakanishi, A., Kishikawa, J. I., Tamakoshi, M., Mitsuoka, K., and Yokoyama, K. (2018). Cryo EM structure of intact rotary H(+)-ATPase/synthase from Thermus thermophilus. *Nat. Commun.* 9, 89. doi:10.1038/s41467-017-02553-6

Nakano, A., Kishikawa, J., Mitsuoka, K., and Yokoyama, K. (2022). Mechanism of ATP hydrolysis dependent rotation of ATP synthases. bioRxiv. doi:10.1101/2022.12.23.521728

Nakano, M., Imamura, H., Toei, M., Tamakoshi, M., Yoshida, M., and Yokoyama, K. (2008). ATP hydrolysis and synthesis of a rotary motor V-ATPase from Thermus thermophilus. *J. Biol. Chem.* 283, 20789–20796. doi:10.1074/jbc.M801276200

Noji, H., Yasuda, R., Yoshida, M., and Kinosita, K., Jr. (1997). Direct observation of the rotation of F1-ATPase. *Nature* 386, 299–302. doi:10.1038/386299a0

Oot, R. A., Kane, P. M., Berry, E. A., and Wilkens, S. (2016). Crystal structure of yeast V1-ATPase in the autoinhibited state. *Embo J.* 35, 1694–1706. doi:10.15252/embj.201593447

Rees, D. M., Montgomery, M. G., Leslie, A. G., and Walker, J. E. (2012). Structural evidence of a new catalytic intermediate in the pathway of ATP hydrolysis by F1-ATPase from bovine heart mitochondria. *Proc. Natl. Acad. Sci. U. S. A.* 109, 11139–11143. doi:10.1073/pnas.1207587109

Roh, S. H., Stam, N. J., Hryc, C. F., Couoh-Cardel, S., Pintilie, G., Chiu, W., et al. (2018). The 3.5-A CryoEM structure of nanodisc-reconstituted yeast vacuolar ATPase Vo proton channel. *Mol. Cell* 69, 993–1004. doi:10.1016/j.molcel.2018.02.006

Saita, E., Suzuki, T., Kinosita, K., Jr., and Yoshida, M. (2015). Simple mechanism whereby the F1-ATPase motor rotates with near-perfect chemomechanical energy conversion. *Proc. Natl. Acad. Sci. U. S. A.* 112, 9626–9631. doi:10.1073/pnas.1422885112

Schep, D. G., Zhao, J., and Rubinstein, J. L. (2016). Models for the a subunits of the Thermus thermophilus V/A-ATPase and *Saccharomyces cerevisiae* V-ATPase enzymes by cryo-EM and evolutionary covariance. *Proc. Natl. Acad. Sci. U. S. A.* 113, 3245–3250. doi:10.1073/pnas.1521990113

Shimabukuro, K., Yasuda, R., Muneyuki, E., Hara, K. Y., Kinosita, K., and Yoshida, M. (2003). Catalysis and rotation of F1 motor: Cleavage of ATP at the catalytic site occurs in 1 ms before 40 degree substep rotation. *Proc. Natl. Acad. Sci. U. S. A.* 100, 14731–14736. doi:10.1073/pnas.2434983100

Sobti, M., Ishmukhametov, R., Bouwer, J. C., Ayer, A., Suarna, C., Smith, N. J., et al. (2019). Cryo-EM reveals distinct conformations of E. coli ATP synthase on exposure to ATP. *Elife* 8, e43864. doi:10.7554/eLife.43864

Sobti, M., Ueno, H., Noji, H., and Stewart, A. G. (2021). The six steps of the complete F(1)-ATPase rotary catalytic cycle. *Nat. Commun.* 12, 4690. doi:10.1038/s41467-021-25029-0

Spetzler, D., York, J., Daniel, D., Fromme, R., Lowry, D., and Frasch, W. (2006). Microsecond time scale rotation measurements of single F1-ATPase molecules. *Biochemistry* 45, 3117–3124. doi:10.1021/bi052363n

Suzuki, K., Mizutani, K., Maruyama, S., Shimono, K., Imai, F. L., Muneyuki, E., et al. (2016). Crystal structures of the ATP-binding and ADP-release dwells of the V(1) rotary motor. *Nat. Commun.* 7, 13235. doi:10.1038/ncomms13235

Tan, Y. Z., Keon, K. A., Abdelaziz, R., Imming, P., Schulze, W., Schumacher, K., et al. (2022). Structure of V-ATPase from citrus fruit. *Structure* 30, 1403–1410.e4. doi:10.1016/j.str.2022.07.006

Toei, M., Gerle, C., Nakano, M., Tani, K., Gyobu, N., Tamakoshi, M., et al. (2007). Dodecamer rotor ring defines H+/ATP ratio for ATP synthesis of prokaryotic V-ATPase from Thermus thermophilus. *Proc. Natl. Acad. Sci. U. S. A.* 104, 20256–20261. doi:10.1073/pnas.0706914105

Vasanthakumar, T., and Rubinstein, J. L. (2020). Structure and roles of V-type ATPases. *Trends Biochem. Sci.* 45, 295–307. doi:10.1016/j.tibs.2019.12.007

Weber, J., and Senior, A. E. (1997). Catalytic mechanism of F1-ATPase. *Biochim. Biophys. Acta* 1319, 19–58. doi:10.1016/s0005-2728(96)00121-1

Yasuda, R., Noji, H., Kinosita, K., Jr., and Yoshida, M. (1998). F1-ATPase is a highly efficient molecular motor that rotates with discrete 120 degree steps. *Cell* 93, 1117–1124. doi:10.1016/s0092-8674(00)81456-7

Yasuda, R., Noji, H., Yoshida, M., Kinosita, K., Jr., and Itoh, H. (2001). Resolution of distinct rotational substeps by submillisecond kinetic analysis of F1-ATPase. *Nature* 410, 898–904. doi:10.1038/35073513

Yokoyama, K., Hisabori, T., and Yoshida, M. (1989). The reconstituted alpha 3 beta 3 delta complex of the thermostable F1-ATPase. *J. Biol. Chem.* 264, 21837–21841. doi:10.1016/s0021-9258(20)88260-x

Yokoyama, K., and Imamura, H. (2005). Rotation, structure, and classification of prokaryotic V-ATPase. *J. Bioenerg. Biomembr.* 37, 405–410. doi:10.1007/s10863-005-9480-1

Yokoyama, K., Muneyuki, E., Amano, T., Mizutani, S., Yoshida, M., Ishida, M., et al. (1998). V-ATPase of Thermus thermophilus is inactivated during ATP hydrolysis but can synthesize ATP. *J. Biol. Chem.* 273, 20504–20510. doi:10.1074/jbc.273.32.20504

Yokoyama, K., Oshima, T., and Yoshida, M. (1990). Thermus thermophilus membrane-associated ATPase. Indication of a eubacterial V-type ATPase. *J. Biol. Chem.* 265, 21946–21950. doi:10.1016/s0021-9258(18)45830-9

Yoshida, M., Muneyuki, E., and Hisabori, T. (2001). ATP synthase - a marvellous rotary engine of the cell. *Nat. Rev. Mol. Cell Biol.* 2, 669–677. doi:10.1038/35089509

Zhao, J., Benlekbir, S., and Rubinstein, J. L. (2015). Electron cryomicroscopy observation of rotational states in a eukaryotic V-ATPase. *Nature* 521, 241–245. doi:10.1038/nature14365

Zhou, A., Rohou, A., Schep, D. G., Bason, J. V., Montgomery, M. G., Walker, J. E., et al. (2015). Structure and conformational states of the bovine mitochondrial ATP synthase by cryo-EM. *Elife* 4, e10180. doi:10.7554/eLife.10180